Three-Dimensional Evaluation of Accommodating Intraocular Lens Shift and Alignment In Vivo

Susana Marcos, PhD,[1] Sergio Ortiz, PhD,[1] Pablo Pérez-Merino, MSc,[1] Judith Birkenfeld, MSc,[1] Sonia Durán, MD,[2] Ignacio Jiménez-Alfaro, MD, PhD[2]

Objective: To quantify 3-dimensionally the anterior segment geometry, biometry, and lens position and alignment in patients before and after implantation of the Crystalens-AO (Bausch & Lomb, Rochester, NY) accommodating intraocular lens (A-IOL).

Design: Prospective, observational study.

Participants: Ten patients (20 eyes) with cataract before and after implantation of the Crystalens-AO A-IOL.

Methods: Custom full anterior segment 3-dimensional (3-D) spectral optical coherence tomography (OCT) provided with quantification tools was used to image the cornea, iris, and natural lens preoperatively and intraocular lens postoperatively. Measurements were obtained under phenylephrine preoperatively and under natural viewing conditions and phenylephrine (for accommodative efforts ranging from 0 to 2.5 diopters [D]) and pilocarpine postoperatively.

Main Outcome Measures: Three-dimensional quantitative anterior segment images, corneal geometry and power, anterior chamber depth (ACD), lens thickness, pupil diameter, A-IOL shift with accommodative effort or drug-induced accommodation, and A-IOL alignment.

Results: Crystalline lens and IOLs were visualized and quantified 3-dimensionally. The average ACD were 2.64±0.24 and 3.65±0.35 mm preoperatively and postoperatively (relaxed state), respectively, and they were statistically significantly correlated (although their difference was not statistically correlated with lens thickness). The A-IOL did not shift systematically with accommodative effort, with 9 lenses moving forward and 11 lenses moving backward (under natural conditions). The average A-IOL shift under stimulated accommodation with pilocarpine was −0.02±0.20 mm. The greatest forward shift occurred bilaterally in 1 patient (−0.49 mm in the right eye and −0.52 mm in the left eye, under pilocarpine). The high right/left symmetry in the horizontal tilt of the crystalline lens is disrupted on IOL implantation. Accommodative IOLs tend to be slightly more vertically tilted than the crystalline lens, with increasing tendency with accommodative effort. Two subjects showed postoperative IOL tilts >9 degrees. Changes in pupillary diameter correlated with pilocarpine-induced A-IOL axial shift. Intermediate accommodative demands (1.25 D) elicited the greater shifts in axial A-IOL location and tilt and pupil diameter.

Conclusions: Quantitative 3-D anterior segment OCT allows full evaluation of the geometry of eyes implanted with A-IOLs preoperatively and postoperatively. High-resolution OCT measurements of the Crystalens 3-D positioning revealed small (and in many patients backward) A-IOL axial shifts with both natural or drug-induced accommodation, as well as tilt changes with respect to natural lens and accommodative effort. *Ophthalmology 2014;121:45-55 © 2014 by the American Academy of Ophthalmology.*

Intraocular lenses (IOLs) that replace the natural crystalline lens in cataract surgery have evolved immensely in the past 40 years. Today, improved IOL designs aim not only at eliminating opacification and refractive errors but also at minimizing ocular aberrations[1,2] or compensating presbyopia (e.g., multifocal IOLs).[3] Multifocal IOLs (expanding depth of focus[4] or providing simultaneous vision[5]) may provide the presbyopic patient with the capability of seeing distance objects and reading without the need of spectacles, but typically at the expense of reducing optical quality at all distances,[6] and do not provide the patient with a true dynamic accommodation capacity.

In the past 10 years, accommodating IOLs (A-IOLs) have been proposed that aim at restoring accommodation. In most cases, changes in the optical power are achieved by moving elements in the IOL that respond to the action of the ciliary muscle on an accommodative demand.[7–9] Some designs claim changes in the curvature of the lens surfaces (e.g., NuLens [NuLens Ltd., Herzliya, Israel][10] and PowerVision [PowerVision Inc., Belmont, CA][11]), although the most

ISSN 0161-6420/14/$ - see front matter
http://dx.doi.org/10.1016/j.ophtha.2013.06.025

common solutions (e.g., Crystalens [Bausch & Lomb, Rochester, NY],[12,13] 1CU Human Optics [Human Optics AG, Erlangen, Germany],[14] Synchrony[15] [Abbott Medical Optics Santa Ana, CA]) are based on axial displacement of the optical element(s) to produce a change in their effective power.

The Crystalens, a prior version of which was developed by Eyeonics Inc. (AT-45; Aliso Viejo, CA)[13] and which is currently commercialized by Bausch & Lomb, was approved by the Food and Drug Administration in 2003 and has been implanted in numerous patients. This A-IOL is biconvex, with flexible hinged-plate haptics that in principle allow a forward or backward movement of the IOL. Most studies of this IOL (or other A-IOLs) primarily report visual functional outcomes in patients who have received the lens (visual acuity in most cases).[12,13,16–22] Although measurements of visual performance are essential to evaluate the safety and efficacy of the IOL, this target outcome may be confounded by several factors and does not provide an understanding of whether the A-IOL is functioning according to its principles of operation. In particular, improved near visual acuity may be the result of increased aberrations, which expand depth of focus (as in a multifocal IOL) rather than a true change in refraction. The amplitude of accommodation also has been used as a target measurement, using both subjective (e.g., push-up or negative lens techniques) and objective (e.g., dynamic photorefraction or aberrometry) methods. The mean amplitude of accommodation reported with the AT-45 was approximately 1 diopter (D)[23] or less (0.44 D),[24] which appears close to the depth of focus of the pseudophakic eye. Subsequent refinements in the designed shape of the Crystalens surfaces (in aspheric optics designs) also play a role in the contribution of the static depth of focus to the potentially dynamically achieved accommodation amplitude.

The most objective way to evaluate whether A-IOLs are operating as expected by design is their direct intraocular visualization. Several studies have used high-frequency ultrasound biomicroscopy (UBM) to visualize the movement of the A-IOL. This technique requires eye immersion and contact with a probe, which may compromise the fixation stability, and the images show a relatively low axial resolution. Although there have been attempts for 3-dimensional (3-D) imaging with custom-developed UBM technology both in vitro and in vivo,[25] most studies solely report the anterior chamber depth (ACD) based on cross-sectional images. With the use of UBM, Marchini et al[23] reported a forward mean shift of 0.32 mm at 1 month (with several eyes showing backward shifts), and Stachs et al[25] reported a forward a mean shift of 0.24 mm under pilocarpine treatment.

Partial coherence interferometry (PCI) is a well-suited technique to measure potential displacements of the IOL on accommodation because of its higher resolution compared with UBM and noncontact nature.[26] However, attempts to actually measure the movement of the Crystalens with PCI are scarce.[27,28] Koeppl et al[27] detected only negligible counterproductive backward movement of the AT-45 with pilocarpine-induced accommodation.

Apart from potential shifts of the Crystalens in the axial direction, observational studies have also reported cases of asymmetric vaulting in the IOL, in the most extreme cases known as "Z syndrome."[29] The lens tilt is likely caused by capsular contraction or asymmetric fibrosis in the haptic region.[30] Measurement of tilt and decentration with this IOL is particularly relevant because the hinged design of the haptic and the effect of accommodative forces onto the lens likely play a role in IOL alignment. Although there are several reports of quantitative, systematic measurements of IOL tilt and decentration in pseudophakic patients implanted with monofocal IOLs using custom-developed methods based on Purkinje or Scheimpflug imaging,[31–33] such measurements have not been performed, to our knowledge, in patients implanted with A-IOLs, the Crystalens in particular.

Quantitative spectral optical coherence tomography (OCT) 3-D full anterior segment geometry and biometry have been presented recently.[34] New swept-source OCT implementations allow the range to be expanded, giving access to 3-D images of the anterior segment from the anterior cornea to the posterior lens with high speed and resolution.[35] Automatic image processing tools along with distortion correction artifacts allow full quantification of the anterior segment from the same instrument, including anterior and posterior corneal topography and pachymetry, pupillometry, ACD, lens surface topography, lens pachymetry, and lens tilt and decentration viewed 3-dimensionally.[36–41] The technique allows true volumetric quantification of the anterior segment (within the pupillary region), greatly surpassing the resolution and quantification capabilities of UBM, and expands to 3-D the 1-dimensional information provided by PCI. Anterior chamber depth is therefore obtained without potential biases produced by the patient fixation variability because the 3-D nature of the measurements allows the consistent measurement of ACD along a clearly identified axis.

Quantitative spectral OCT is therefore a suitable technique to quantify the performance of A-IOLs, by full characterization of IOL positioning 3-dimensionally, with respect to the preoperative crystalline lens and as a function of accommodative effort because of its high resolution, unequivocal references, and breadth of provided quantitative information. The 3-D anatomic information provided by OCT can be used to build custom eye models[42] that help to understand the impact of the structural properties of the eye (corneal shape, lens design, biometry, lens alignment) on optical performance, in particular with A-IOLs at different accommodation stimuli.

In this study, we applied quantitative spectral OCT 3-D biometry in a group of 20 eyes implanted with the Crystalens-AO preoperatively and postoperatively to quantify the structural changes in cataractous eyes on implantation of the Crystalens and to quantify 3-dimensionally the changes in IOL position on accommodative demand.

Methods

This study was conducted in accordance with the principles of the Declaration of Helsinki and good clinical practice. All protocols were approved by the institutional review boards at Fundación Jiménez Díaz (FJD) and Consejo Superior de Investigaciones Científicas. Patients signed informed consents after being appropriately informed of the nature of the study.

Table 1. Profile of Eyes in the Study

Age (yrs)	75.22±4.39
Male/female	1/9
Right eye/left eye	10/10
Preoperative sphere (D)	+0.78±2.34
Preoperative cylinder (D)	−1.14±0.67
Preoperative K (D)	44.16±1.17
Preoperative axial length (mm)	23.07±0.74
IOL power (D)	22.29±1.77

Value are shown as n/n and mean ± standard deviation.
D = diopter; IOL = intraocular lens; K = corneal curvature.

Patients

Sequential patients from the FJD who met the inclusion criteria, presented good general health with no pre-existing ocular pathology, and were referred to cataract surgery were invited to participate in the study. The inclusion criteria included age ≥50 years, with manifest astigmatism <1.5 D, with bilateral cataract considered as the sole cause of visual acuity decrease. A total of 21 eyes from 11 patients were studied. Quantitative reports are given for the 20 eyes from 10 patients in whom data on both right and left eyes were available. Patients underwent surgery and had clinical evaluation at FJD and were evaluated preoperatively and postoperatively (3 months) at the Visual Optics and Biophotonics Laboratory (Institute of Optics, Consejo Superior de Investigaciones Científicas). Table 1 shows the profile of the studied patients.

Intraocular Lenses

Patients received the Crystalens-AO implant, which is a 3-piece plate haptic lens with a biconvex single-optic design. The haptics are rectangular plates with hinges close to the optical zone of the lens and polyamide loops. This IOL has aspheric surfaces (nominally aiming at zero IOL aberration). The IOL is of biocompatible third-generation silicone (Biosil) with a refraction index of 1.428. The IOL power was selected using the SRK/T or the Holladay II formula, using biometric data from the IOLMaster (Carl Zeiss Meditec, Dublin, CA) and A-constant = 119.10. The power of the implanted IOLs ranged from 19.50 to 24.50 D. Preoperative and postoperative spherical and cylindrical errors were obtained from subjective refractions.

Surgical Technique

All surgeries were performed by the same surgeon (S.D. at FJD) using a standard phacoemulsification technique under local anesthesia (topical preservative-free lidocaine 1% or peribulbar injection). The IOLs were implanted using an injector designed for that purpose. Clear sutureless corneal incisions were created in superior/temporal and superior/nasal locations in the right and left eyes, respectively, and enlarged to approximately 2.8 mm. Anterior curvilinear capsulorhexis (6.5 mm intended diameter) was created manually. The achieved size and centration of the capsulorhexis and the haptic orientations were checked postoperatively using en face OCT images under pupil dilation.

All patients received standard postoperative treatment with topical steroids and antibiotics. Topical atropine 1% was instilled at the end of surgery and on the first postoperative day to paralyze the ciliary muscle, with the aim of fixating the IOL in the most posterior position in the capsular bag during the early stages of capsular fibrosis. All surgeries were uneventful, and all IOLs were successfully implanted intracapsularly.

Quantitative Anterior Segment Spectral Optical Coherence Tomography

A custom-developed OCT instrument was used to image the full anterior segment of the eye 3-dimensionally. This development was the result of a collaborative effort between the Institute of Optics and Copernicus University. The system has been described in prior publications.[34,38] In brief, the set-up is based on a Michelson interferometer configuration with a superluminescent diode (central wavelength, 840 nm; bandwidth, 50 nm) and a spectrometer (diffraction grating and a complementary metal-oxide semiconductor camera as a detector). The effective acquisition speed is 25.000 A-scans/second. The axial range of the instrument is 7 mm, with a theoretic axial pixel resolution of 3.4 μm.

The system is provided with fan and optical distortion correction, which compensate for the distortions produced by the scanning architecture of the instrument[36,38] and the distortion produced by the refraction from the preceding optical surfaces.[37] The automatic image processing tools for de-noising, segmentation, clustering, merging, and biometric and IOL alignment measurements have been described in detail.[40,41] The quantification capabilities of the instrument have been demonstrated with artificial model eyes with known dimensions, in vitro and in vivo measurements, and comparisons with other instruments (videokeratoscopy, Scheimpflug, Purkinje imaging, and noncontact profilometry).

For the purposes of this study, a motorized Badal system to stimulate accommodation was incorporated in the fixation channel. Fixation is provided by a mini-display, which allows projection of accommodating targets. The desired accommodative demand was produced by changing the distance between the 2 lenses of the Badal system, which allowed a change in vergence while keeping constant retinal and pupil magnification. A similar motorized Badal system had been validated in a custom-developed Hartmann-Shack system. This dynamic aberrometer allowed direct measurements of the accommodative response, which matched well the accommodative demand in young subjects, particularly when their aberrations were corrected by adaptive optics.[43] The motor was moved in synchronization with the image acquisition program in the OCT system.

Experimental Procedures

Spectral OCT anterior segment images were acquired preoperatively and postoperatively. Preoperative measurements were conducted under natural conditions for relaxed accommodation. Postoperative measurements were typically conducted in 2 sessions. In a first session, measurements were obtained under natural conditions (which allowed monitoring of the natural pupil diameter) and then 30 minutes after instillation of 1% pilocarpine to pharmacologically stimulate accommodation. In a second session, measurements were obtained under instillation of phenylephrine, which allowed larger pupils, and therefore a wider view of the IOL, without paralyzing the ciliary muscle.

Patients were stabilized by means of a bite bar and asked to fixate their gaze on the text (20/25 Snellen E-letters) in the fixation channel mini-display (SVGA OLED LE400; Liteye Systems, Inc., Centennial, CO). The position of the fixating letters was moved across the display until the cornea was aligned with the optical axis of the instrument. To achieve a full 3-D anterior segment image, 3 images (50 B-scans, composed of a collection for A-scans in a 7×15-mm lateral area), with the OCT beam focused in the cornea and anterior and posterior lens, were obtained sequentially. Three accommodative demands (0, 1.25, and 2.5 D) were produced with the Badal optometer, and the patient was requested to focus the text on the display. Three full anterior segment images were obtained per accommodation condition. Each image was obtained in

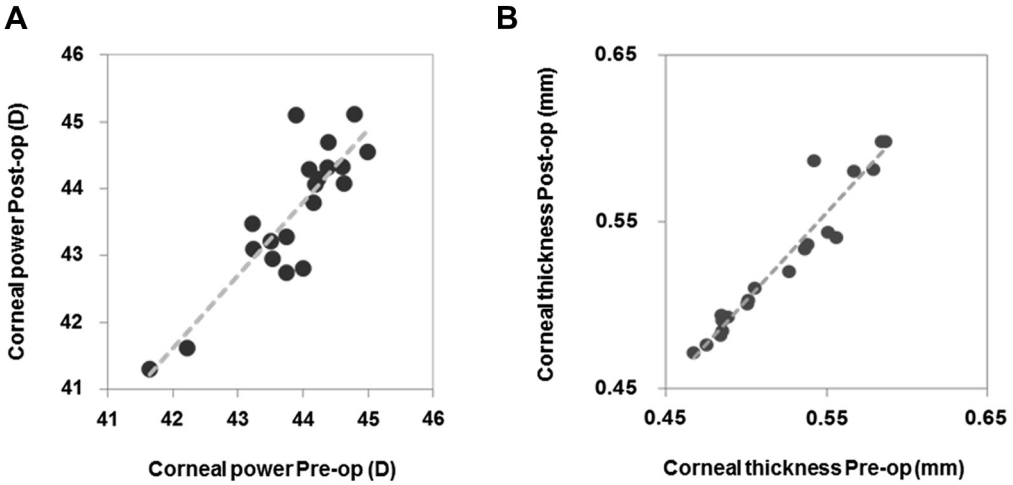

Figure 1. **A**, Preoperative corneal power versus postoperative corneal power computed from spectral optical coherence tomography anterior and posterior corneal surface shapes. **B**, Preoperative (pre-op) versus postoperative (post-op) corneal thickness. D = diopter.

0.72 seconds. Image collection protocols were similar in the natural viewing and phenylephrine conditions. Collection of all images for each condition typically took approximately 30 minutes. The pilocarpine condition involved acquisition of only 1 series of images for a fixed position of the Badal optometer.

Outcome Measures

Anterior and Posterior Corneal Shape. The anterior and posterior corneal elevation maps are obtained from the anterior and posterior surfaces from automatically segmented and corrected spectral OCT images and, for the purposes of this study, fitted to spheres. The mean corneal curvature was obtained from the apical mean anterior and posterior radius of curvature, assuming a corneal index of refraction of 1.376.

Three-Dimensional Reconstructions of Full Anterior Segment. Full anterior segment images (from the anterior corneal surface to the posterior lens surface) were obtained preoperatively and postoperatively. Automatic clustering analysis allowed automatic identification of the cornea, iris, and lens. The iris plane and 3-D coordinates of the pupil center were used to register preoperative and postoperative anterior segment images in the same eye as well as postoperative anterior segment images in the same eye for different accommodative demands. Because of the high accuracy of image registration, the cornea and iris appear merged across conditions.

Anterior Chamber Depth. The ACD was obtained from the spectral OCT data as the distance between the posterior corneal apex and the anterior lens surface apex. In contrast to ACD obtained from a single A-scan (as in PCI), ACD is consistently measured along the same axis independent of the fixation stability of the subject.

Natural Lens Thickness. The crystalline lens thickness was obtained from spectral OCT data as the distance between the anterior and posterior lens vertex.

Intraocular Lens Tilt. Crystalline lens/IOL tilt was obtained from spectral OCT data as the angle between the axis of the lens and the pupillary axis. The lens/IOL axis is defined as the vector that joins the apexes of the anterior and posterior lens surfaces apexes. The pupillary axis is defined as the vector that joins the center of curvature of the anterior cornea and the pupil center. Crystalline lens and IOL tilt were computed for preoperative and postoperative (all accommodative demands) measurements under phenylephrine.[41,44]

Pupillometry. Pupil diameter was obtained from corrected spectral OCT images by fitting of the iris to an ellipse. Pupil diameter was studied in postoperative measurements under natural conditions.

Capsulorhexis and Haptic Axis. The margins of the capsulorhexis and the locations of the haptics were identified from en face OCT images obtained under phenylephrine pupil dilation. The diameter and centration (with respect to the lens optical zone) of the capsulorhexis were estimated by circumference fitting. In addition, the polar coordinates of the haptics were obtained by estimating the axes of the visualized haptics (0 degrees indicating a horizontal axis, 90 degrees indicating a vertical axis, and 135 degrees indicating temporal/superior and nasal/superior axes in the right and left eyes, respectively).

Results

Corneal Shape

Figure 1 shows preoperative and postoperative corneal power and corneal thickness. Preoperative and postoperative corneal parameters were highly correlated. There was a high repeatability in corneal power (0.063-mm standard deviation, on average, across subjects and conditions, preoperatively and postoperatively) and corneal thickness (3.8-μm average standard deviation). Also, there were no statistically significant differences in corneal power preoperatively and postoperatively or in corneal thickness (except for S#10-OS, $P<0.05$).

Three-Dimensional Reconstructions of Full Anterior Segment

Videos 1 and 2 (available at http://aaojournal.org) show 3-D images of the full anterior segment. Video 1 (available at http://aaojournal.org) represents a merged preoperative and postoperative 3-D image showing both the crystalline lens and the implanted IOL (relaxed accommodation) with phenylephrine in patient S#8-OD. The relative 3-D position of the IOL with respect to the natural lens can be observed. The anterior surface of the IOL sits 0.71 mm behind the anterior surface of the preoperative natural crystalline lens and is tilted more superiorly.

Video 2 (available at http://aaojournal.org) represents a merged postoperative 3-D image showing the crystalline implanted IOL for 3 accommodative demands (0, 1.25, and 2.5 D) in patient S#11

(under natural conditions), with the IOL volume depicted in different colors for each accommodation. The IOL moved backward with accommodation (by 700 μm from 0 to 2.5 D of accommodation), and changes in tilt and decentration are not observed in this eye. Snapshots of the 3-D rendering shown in Videos 1 and 2 (available at http://aaojournal.org) are displayed in Figure 2E and Figure 3C, respectively.

Anterior Chamber Depth

Average ACD was 2.64±0.24 mm preoperatively and 3.65±0.35 mm postoperatively (relaxed accommodation). Measurements of ACD were highly reproducible (average standard deviation of repeated measurements of 0.015 mm preoperatively and 0.035 mm postoperatively). Independent measurements of ACD postoperatively with dilated pupils under phenylephrine and natural conditions were not statistically significantly different. There was a high statistical correlation of ACD between the right and left eyes preoperatively ($r = 0.9342$; $P = 0.0001$; Fig 2A). The correlation was still significant postoperatively ($r = 0.9276$, $P = 0.0032$ for measurements with phenylephrine; $r = 0.8397$, $P = 0.0123$ for measurements under natural conditions; Fig 2B), excluding S#3, which consistently showed high postoperative ACD values (4.46 mm) in the left eye. There was a statistically significant correlation between preoperative and postoperative ACD ($r = 0.438$, $P<0.0001$ for measurements with phenylephrine; and $r = 0.399$; $P<0.0001$ for measurements under natural conditions; Fig 2C). We found a highly significant correlation between postoperative ACD and postoperative spherical equivalent ($r = 0.655$; $P = 0.0017$). Interocular (right/left eye) differences in ACD also were significantly correlated with interocular differences in spherical equivalent ($r = 0.713$; $P = 0.02$).

Changes in Anterior Chamber Depth with Accommodative Effort

There was not a consistent shift of the A-IOL with accommodative effort. The A-IOLs shifted on average by +0.005±0.025 mm for an accommodative effort of 1.25 D and +0.008±0.03 mm for an accommodative effort of 2.5 D under phenylephrine and −0.006±0.036 and +0.01±0.02 mm, respectively, under natural conditions. The average A-IOL shift under stimulated accommodation with pilocarpine was −0.02±0.20 mm. The measured A-IOL shift values are above the accuracy of the technique but clinically not significant. Figure 3 shows the relative shifts of the A-IOL as a function of accommodative effort in the right and left eyes of all patients under both phenylephrine (Fig 3A) and natural conditions (Fig 3B). The postoperative ACD measured under pilocarpine accommodation is also shown for reference. Some eyes (8 under phenylephrine and 9 under natural conditions) experienced a forward move of the A-IOL with accommodative effort (1.25 D of accommodative stimulus), as expected from design, whereas others moved backward. In general, a greater shift (in absolute values) was elicited by the 1.25-D accommodative stimulus than by a 2.5-D accommodative stimulus (thus, the V or inverted V-shape of the shift vs. accommodative stimulus functions in Fig 3). With pilocarpine, 8 A-IOLs moved forward (−0.19±0.22 mm, on average) and 12 A-IOLs moved backward (+0.09±0.22 mm, on average). We did not find a significant correlation between the A-IOL shift in the right and left eyes (under phenylephrine or under natural conditions). The correlation between the pilocarpine-induced A-IOL shift in the right and left eyes was statistically significant ($r = 0.843$; $P = 0.0023$). However, the A-IOL shift was relevant in both eyes (−0.49 and −0.52 mm in the right and left eyes, respectively) only in S#6.

Natural (and Phenylephrine) Accommodation Versus Pilocarpine-Induced Accommodation

Figure 2D shows the postoperative ACD measured (for all accommodative stimuli) under phenylephrine versus natural accommodation. There is a highly statistical significant correlation ($r = 0.99$; $P<0.0001$) between the 2 types of data (obtained in different sessions). Compared with intersubject differences, the relative shift of the A-IOL with stimulated accommodation is almost negligible. We did not find significant correlations between the A-IOL shifts under phenylephrine or natural accommodation. Likewise, we did not find overall significant correlations between A-IOL shift under natural (or phenylephrine) accommodation and pilocarpine-induced accommodation, likely because of the small amount of effective A-IOL shifts. However, in 5 eyes, we found consistent shift signs in both natural and pilocarpine-induced accommodation.

Pupil Diameter Changes

The natural pupil diameter was highly correlated between the right and left eyes in the relaxed accommodation state ($r = 0.827$; $P = 0.0032$; Fig 4A). The changes in pupil diameter (natural accommodation measurements) with accommodative effort were also symmetric between the right and left eyes ($r = 0.617$; $P = 0.0038$; Fig 4B). In keeping with the nonprogressive response of A-IOL shift with accommodative effort, the pupil diameter change was typically nonprogressive with accommodative effort with neither the V nor the inverted-V pattern in most subjects. The change in pupil diameter with accommodative effort was not positively correlated with A-IOL shift (in natural conditions), although we found a statistically significant correlation between change in pupil diameter and pilocarpine-induced A-IOL shift ($r = 0.489$, $P = 0.0286$ and $r = 0.454$, $P = 0.045$ for pupil diameters at 1.25 D and 2.5 D stimuli, respectively). Several subjects experienced a slight increase in pupil diameter with accommodative effort (Fig 5). On average, pupil diameter changed by +0.041±0.15 mm for a 1.25-D accommodative effort and by −0.015±0.21 mm for a 2.5-D accommodative effort. Only 7 eyes showed a consistent pupillary miosis with accommodation.

Lens Thickness

Average preoperative crystalline lens thickness was 4.53±0.22 mm. The standard deviation of repeated lens thickness measurements was 0.030 mm (averaged across eyes). Preoperative lens thickness was highly correlated between the right and left eyes ($r = 0.79$; $P = 0.006$; Fig 6). However, we did not find an association between preoperative lens thickness and A-IOL shift in any of the conditions being tested. Preoperative lens thickness was not statistically correlated with the difference of preoperative and postoperative ACD.

Lens Tilt

Lens tilt was measured with reproducibility of 0.79 degrees around the x-axis and 0.44 degrees around the y-axis. There were no differences in the measurement reproducibility among the crystalline lens, A-IOL, and different accommodative efforts. The lens average tilt magnitude was 5.71 degrees preoperatively (crystalline lens) and 5.01 degrees postoperatively (A-IOL, relaxed accommodation). The intersubject variability in lens tilt was lowest for the natural lens (standard deviation, 1.30 degrees) and highest for the A-IOLs with increasing accommodative effort (2.46, 3.02, and 3.19 degrees for A-IOL at 0, 1.25, and 2.5 D of accommodative effort, respectively). Figure 7 shows the horizontal and vertical coordinates of tilt in the right and left eyes both preoperatively and postoperatively (phenylephrine, all accommodative efforts).

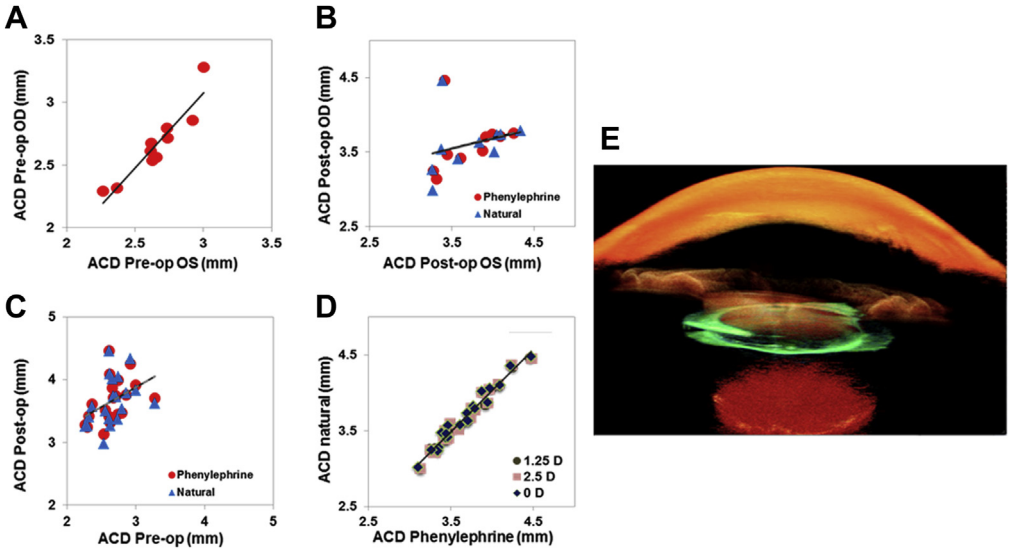

Figure 2. **A**, Preoperative (pre-op) anterior chamber depth (ACD) in left versus right eye. **B**, Postoperative (post-op) ACD in left versus right eye (under natural and phenylephrine conditions). **C**, Preoperative versus postoperative ACD (under natural and phenylephrine conditions). **D**, Postoperative ACD under natural conditions (for different accommodative demands) versus postoperative ACD under phenylephrine stimulation. **E**, Three-dimensional view of merged full anterior segment 3-dimensional optical coherence tomography images in the same patient before and after Crystalens (Bausch & Lomb, Rochester, NY) accommodating intraocular lens implantation. OD = right eye; OS = left eye.

Preoperatively the crystalline lens was systematically tilted around the vertical axis by 5.1 degrees, on average, with the nasal side of the lens forward (positive right eye). Also, the lens tends to tilt around the horizontal axis (by 1.96 degrees, on average) with the superior side of the lens moved forward. There is a high mirror symmetry in natural lens tilt between the left and right eyes ($r = 0.847$; $P = 0.0019$). The nasal/temporal symmetry between left and right eye IOL tilt is lost postoperatively (relaxed accommodation) ($r = 0.237$; $P = 0.5$). The nasal side of the lens IOLs tilted further backward in 2 eyes and tilted forward in 8

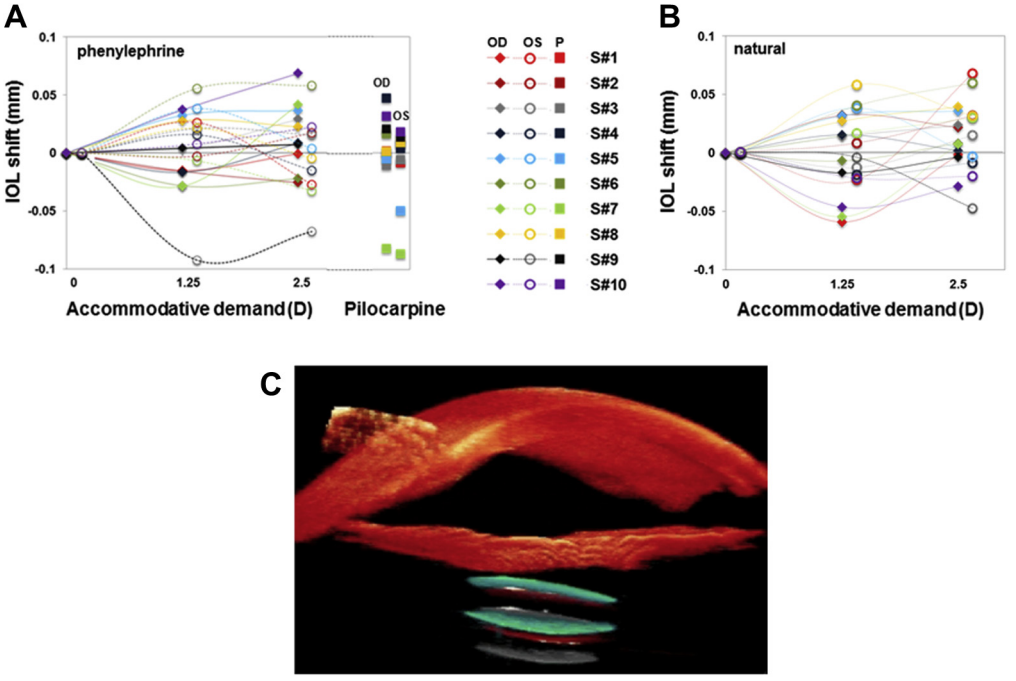

Figure 3. Relative shift of the accommodating intraocular lens (A-IOL) as a function of accommodative demand (*solid diamonds*, right eyes; *open circles*, left eyes) and pilocarpine stimulation (*solid squares*; P in the legend). Positive shifts indicate backward A-IOL movement and negative shift indicates forward lens movement. Phenylephrine conditions (**A**), natural conditions (**B**), and 3-dimensional (3-D) view of merged full anterior segment image 3-D optical coherence tomography postoperatively in the same patient implanted with the Crystalens A-IOL for 3 different accommodative efforts (**C**). D = diopters; IOL = intraocular lens; OD = right eye; OS = left eye.

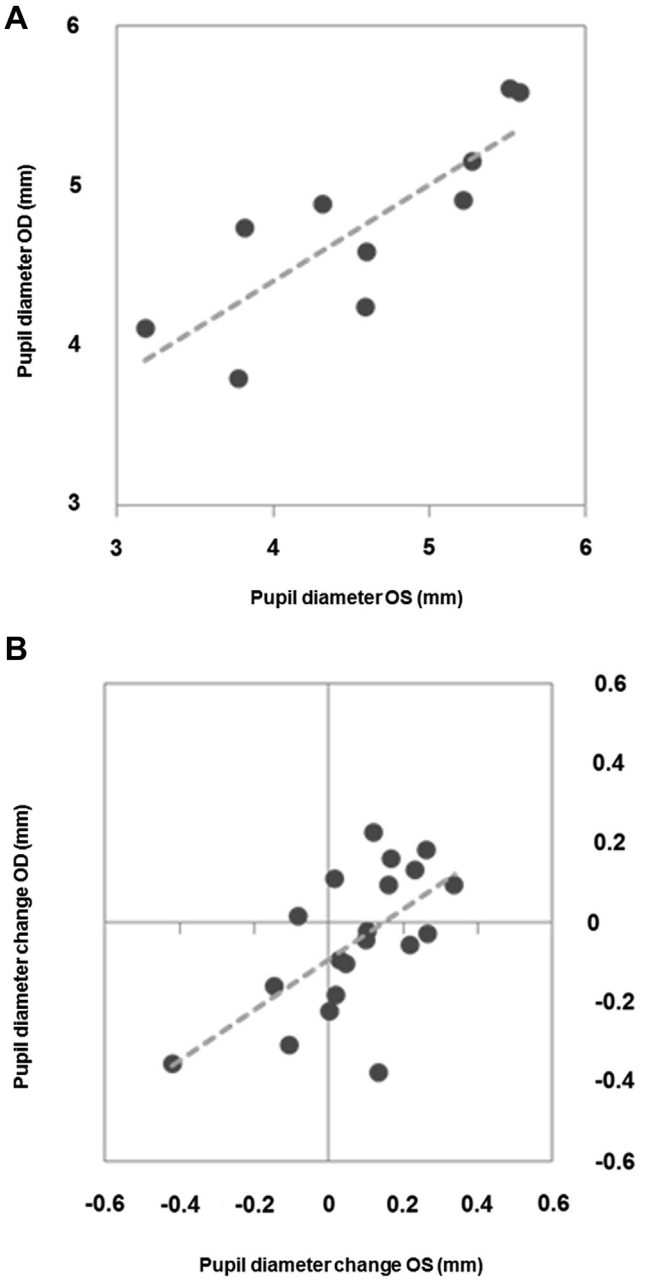

Figure 4. **A**, Preoperative pupil diameter in the left versus right eye. **B**, Postoperative changes in pupil diameter under natural accommodation (difference of pupil diameter under relaxed accommodation and for 1.25 D of accommodative demand) in the left versus right eye. OD = right eye; OS = left eye.

eyes. There is a slight trend for the superior side of the lens to move further backward. Two eyes (S#9-OD and S#10-OS) experienced large shifts in IOL alignment with respect to the natural lens, showing tilts around y of more than 9 degrees for the relaxed state of accommodation.

Figure 7 shows A-IOL tilt around *x*-axis and *y*-axis as a function of accommodative effort in all eyes. Although the tilt around y-axis (nasal/temporal tilt) remained fairly constant with accommodative effort, the tilt around *x*-axis (superior/inferior) varied significantly with accommodative effort in most eyes showing the characteristic V/inverted V-patterns found in other parameters (A-IOL shift and pupil diameter) with accommodative effort. The superior side of the IOL moved backward in 12 eyes and forward with accommodative effort in 8 eyes. On average, the IOL tilted around the *x*-axis 1.65 degrees for 1.25 D and 1.53 degrees for 2.5 D of accommodative effort. The greatest A-IOL tilt change (9.5 degrees) during accommodative effort occurred for S#1-OS. There was no correlation between the relative tilt of the implanted A-IOL (relaxed state) with respect to the natural lens and the change with accommodation.

Capsulorhexis and Haptic Axis

The average measured capsulorhexis diameter was 4.88±0.72 mm (3 months postoperatively). The capsulorhexis was generally elliptical in shape and slightly smaller than the intended diameter, likely because of fibrosis-induced shrinkage. The magnitude of the capsulorhexis shifts with respect to the IOL center was 0.34±0.30 mm on average. Horizontal shifts ranged from 0.22 mm temporal to 0.63 mm nasal in the right eye and were consistently temporal in the left eye; vertical shifts ranged from 1.33 mm superior to −0.63 mm inferior. In the left eye, the greatest tilts tended to occur for the greatest capsulorhexis diameters and capsulorhexis shifts. No significant correlation was found between the direction of capsulorhexis shift and the tilt orientation.

The average haptic polar orientation was 129.95±20.38 degrees, consistent with the 120 degrees (11 o'clock) incision location, in both left and right eyes. We did not find significant correlations between horizontal and vertical components of the haptic polar orientations and the measured tilts around horizontal and vertical axes. Tilt changes with accommodation tended to correlate with slight polar rotations in the lens (up to 6.9 degrees).

Discussion

Custom-developed 3-D full anterior segment OCT has allowed a comprehensive quantitative evaluation of the anterior segment in patients with cataract and after implantation of the Crystalens-AO A-IOL. To our knowledge, this is the first time that lens alignment has been measured before and after cataract surgery and that quantitative OCT has been used in a series of patients to assess corneal geometry, biometry, and lens tilt of A-IOLs, particularly under the natural response to an accommodative stimulus and induced by pilocarpine. All measurements were obtained using the same instrument, which has shown excellent reproducibility.

There are several reports in the literature reporting the outcomes of different versions of the Crystalens A-IOL by Bausch & Lomb or the prior AT-45 design by Eyeonics Inc. Although the literature is relatively extensive in assessing visual performance at various distances, few studies evaluate the actual shifts of the lens within the eye. Measurement of those shifts and their potential relationships with other physical parameters is essential in understanding the mechanism of operation of the lens and its optical outcomes.

We found small axial shifts of the A-IOL with natural or stimulated accommodation. The average displacement was negligible in all cases. Several subjects showed a forward movement of the A-IOL (the greatest forward shift was close to 0.5 mm in both eyes in 1 subject with pilocarpine

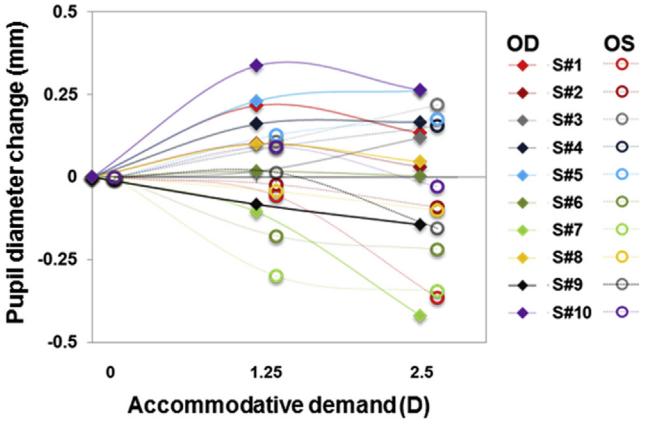

Figure 5. Pupil diameter change as a function of accommodative demand. D = diopter; OD = right eye; OS = left eye.

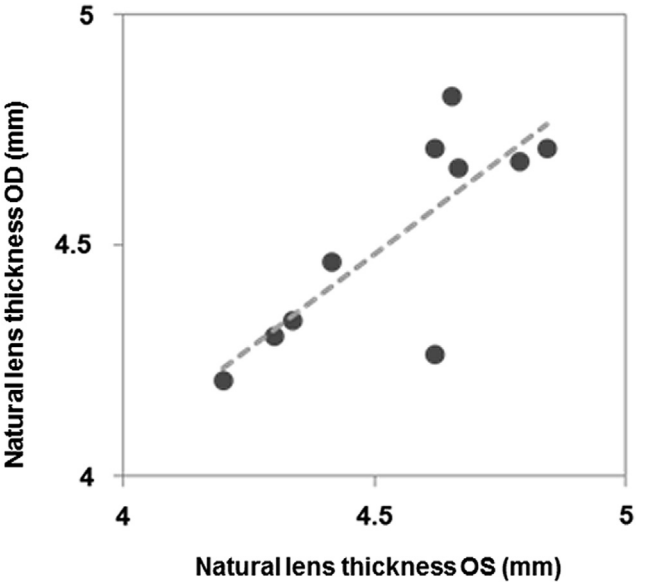

Figure 6. Preoperative lens central thickness in the left versus right eye. OD = right eye; OS = left eye.

and under natural accommodation). The average forward shift with pilocarpine-induced accommodation was 0.28 mm, and the average backward shift was 0.09 mm. These values are close to previous reports of pilocarpine-induced A-IOL shifts, from Koeppl et al,[27] using PCI in 28 eyes implanted with the Crystalens AT-45 (who reported an average backward shift of 0.136 mm) and from Stachs et al,[24] using custom-developed 3-D UBM in 4 patients who received the Crystalens AT-45 (who reported an average forward shift of 0.13 mm). Those A-IOL axial shifts are too small to produce a clinically relevant dioptric shift.

Measurements under natural accommodative effort (and not only pilocarpine-induced effort) allowed us to assess the response of the lens to a natural accommodative stimulus. In most patients, the greatest variation occurs with a 1.25-D accommodative response, which suggests that the near target elicits a response in the ciliary muscle, although the lack of effective focusing on the retina may prevent extending the effort in response to higher dioptric stimuli (2.5 D). The correlation of the changes in A-IOL position with the changes in pupil diameter on accommodation is also suggestive of the activation of the accommodative response on the stimulus. Of note, consistent pupillary miosis with increased accommodative effort occurred in only a few subjects (and most notably in the subject who

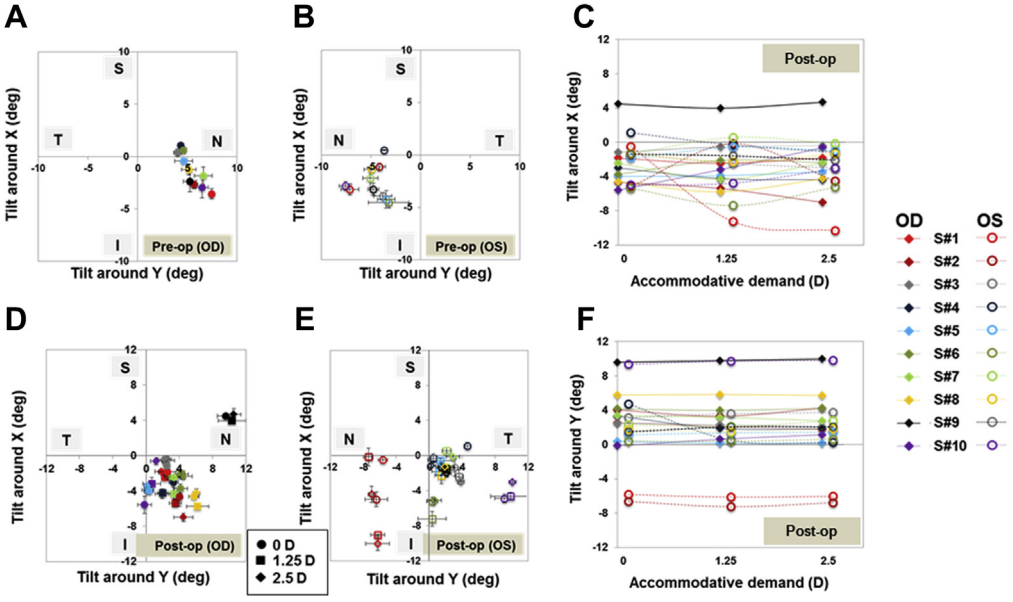

Figure 7. Preoperative (**A, B**) and postoperative (**C, D**) lens tilt coordinates on right (**A, C**) and left (**B, D**) eyes. **E**, The accommodating intraocular lens (A-IOL) tilt around x (superior/inferior). **F**, The A-IOL tilt around y (nasal/temporal). Tilts around x represent superior/inferior tilts. Tilts around y represent nasal/temporal tilts. D = diopter; OD = right eye; OS = left eye.

experienced the greatest A-IOL forward shift under both natural conditions and pilocarpine). The observed slight increase in pupil diameter in some subjects seems contradictory to the expected accommodative response, but the association with the reversed shift of the A-IOL in these patients remains unclear. In any case, the lack of pupillary miosis response in young subjects with normal accommodative responses has been reported in the literature,[45] so it is not unlikely that this also may occur in presbyopic and pseudophakic patients.

The correlation of the biometric measurements preoperatively and postoperatively gives some interesting insights on the mechanism of the A-IOL. As expected, ACD and lens thickness are highly correlated in the right and left eyes preoperatively. The right−left correlation of ACD postoperatively indicates that the overall axial position of the A-IOL is driven by anatomic parameters, primarily the size of the anterior segment, as previously suggested for monofocal IOLs.[46] However, we did not find a fine-tuning of the IOL location (in relaxed accommodation) within the capsular bag. In patients implanted with monofocal IOLs, Olsen[46] found that the postoperative ACD is linearly related with the preoperative ACD and lens thickness and used this as a predictor for the estimated lens position through the C-constant, which would account for the role of haptic angulation and biomechanical features of the IOL platform in the actual axial location of the IOL. We could not determine a C-constant for these lenses (because of the high dispersion of the correlation of before and after ACD vs. lens thickness), which suggests that the lens does not sit at a well-defined location within the lens capsule, likely as the result of the hinged haptic design; therefore, its axial position in a relaxed accommodation state cannot be finely defined. In addition, we could not establish a correlation between lens thickness and A-IOL shift, which suggests that other factors beyond the lens anatomy (e.g., capsular fibrosis) play a role in the ability of the A-IOL to move within the eye and in the direction of displacement.

Quantitative 3-D OCT also allowed accurate measurements of the A-IOL tilt both preoperatively and postoperatively at different accommodative demands. Although IOL tilt has been measured before in young normal eyes and in eyes implanted with IOLs using Purkinke or Scheimpflug imaging, this is, to our knowledge, the first time that these measurements have been performed on the same eyes with the natural lens and after its replacement by an IOL. Knowledge of the relative location of the implanted A-IOL within the capsular bag and potential changes with accommodation provide additional insights into the mechanism of the A-IOL. As previously reported,[32] we found a nasal-temporal tilt of the natural lens (~5 degrees on average) that was highly symmetric across left and right eyes. Although the left−right symmetry of lens tilt and decentration occurs in some eyes (as previously reported in pseudophakic eyes implanted with monofocal IOLs), the lack of a general symmetric pattern, changes in orientation of the lens tilt, and the presence of large relative lens tilts (with respect to the preoperative lens orientation) indicate a certain degree of instability in the A-IOL alignment, likely because of the hinged nature of the haptics in this lens. Cases of large IOL tilts in patients with the Crystalens implant have been reported in the literature, known as "Z syndrome."[29] We also found a significant increase in lens tilt with accommodative effort. This tilt occurs primarily around the *x*-axis (superior/inferior tilt), closer to the orientation of the hinged IOL haptics. However, we did not find a significant correlation between the haptic axis coordinates and the tilt coordinates or between the size or decentration of the capsulorhexis and the coordinates of tilt. In the left eye, trends were found between the capsulorhexis diameter and decentration magnitude and the magnitude of IOL tilt. Asymmetric fibrosis is likely to play a role on this effect. Incidentally, the location of the incision (and therefore the haptic axis) seems to play a critical role in the tilt outcomes. The nonmirror symmetric location of the incision (temporal in the right eye and nasal in the left eye) may be related to the disrupture of the right/left eye lens tilt symmetry that was found in the natural lens. In the right eye, the nasal-inferior lens tilt coordinates of the natural lens tends to be preserved postoperatively, but in the left eye, the variability in tilt around the *y*-axis is largely increased, perhaps reflecting tensions between the natural orientation of the capsular bag and the lens axis location. Future studies will correlate anatomic parameters (IOL tilt, incision location) with aberration measurements. In addition, measurements of optical aberrations in these eyes will allow predictions of depth of focus in each eye. An increase in tilt-induced coma might cause an increase in depth of focus, which may facilitate near tasks.

In conclusion, full 3-D quantitative OCT imaging allowed characterization of the anterior segment geometry preoperatively and postoperatively (anterior and posterior corneal surface geometry, ACD, lens geometry, and lens alignment), giving insights on the performance of implanted A-IOLs (Crystalens) on an accommodative stimuli. The axial shifts of the A-IOL were small, and in many cases the lens shifted backward (opposite to the expected movements) on accommodative effort. This indicates that the claimed working mechanism of the Crystalens-AO A-IOL is not by an axial shift. Significant IOL tilts occurred (particularly around the horizontal axis), consistent with the orientation of the hinged haptics. The quantitative anatomic data, all obtained from the same instrument, can be used to obtain customized eye models both preoperatively (for ray tracing calculations of the IOL power, among others) and postoperatively to assess the optical performance of the eye.

References

1. Marcos S, Barbero S, Jiménez-Alfaro I. Optical quality and depth-of-field of eyes implanted with spherical and aspheric intraocular lenses. J Refract Surg 2005;21:223–35.
2. Barbero S, Marcos S, Montejo J, Dorronsoro C. Design of isoplanatic aspheric monofocal intraocular lenses. Opt Express [serial online] 2011;19:6215–30. Available at: http://www.opticsinfobase.org/oe/fulltext.cfm?uri=oe-19-7-6215&id=210901. Accessed June 11, 2013.
3. Leyland M, Zinicola E. Multifocal versus monofocal intraocular lenses in cataract surgery: a systematic review. Ophthalmology 2003;110:1789–98.

4. Piers PA, Fernandez EJ, Manzanera S, et al. Adaptive optics simulation of intraocular lenses with modified spherical aberration. Invest Ophthalmol Vis Sci 2004;45:4601–10.
5. de Gracia P, Dorronsoro C, Sánchez-González A, et al. Experimental simulation of simultaneous vision. Invest Ophthalmol Vis Sci 2013;54:415–22.
6. De Vries NE, Nuijts RM. Multifocal intraocular lenses in cataract surgery: literature review of benefits and side effects. J Cataract Refract Surg 2013;39:268–78.
7. Glasser A. Restoration of accommodation: surgical options for correction of prebyopia. Clin Exp Optom 2008;91:279–95.
8. Dick HB. Accommodative intraocular lenses: current status. Curr Opin Ophthalmol 2005;16:8–26.
9. Sheppard AL, Bashir A, Wolffsohn JS, Davies LN. Accommodating intraocular lenses: a review of design concepts, usage and assessment methods. Clin Exp Optom 2010;93:441–52.
10. Ben-nun J. The NuLens accommodating intraocular lens. Ophthalmol Clin North Am 2006;19:129–34, vii.
11. Nichamin LD, Scholl JA. Shape-changing IOLs: PowerVision. In: Chang DF, ed. Mastering Refractive IOLs: The Art and Science. Thorofare, NJ: SLACK Inc.; 2008:220–2.
12. Cumming JS. Performance of the Crystalens [letter]. J Refract Surg 2006;22:633–4; author reply 634−5.
13. Cumming JS, Colvard DM, Dell SJ, et al. Clinical evaluation of the Crystalens AT-45 accommodating intraocular lens: results of the U.S. Food and Drug Administration clinical trial. J Cataract Refract Surg 2006;32:812–25.
14. Claoué C. Functional vision after cataract removal with multifocal and accommodating intraocular lens implantation: prospective comparative evaluation of Array multifocal and 1CU accommodating lenses. J Cataract Refract Surg 2004;30:2088–91.
15. McLeod SD, Vargas LG, Portney V, Ting A. Synchrony dual-optic accommodating intraocular lens. Part 1: optical and biomechanical principles and design considerations. J Cataract Refract Surg 2007;33:37–46.
16. Alió JL, Piñero DP, Plaza-Puche AB. Visual outcomes and optical performance with a monofocal intraocular lens and a new-generation single-optic accommodating intraocular lens. J Cataract Refract Surg 2010;36:1656–64.
17. Beiko GH. Comparison of visual results with accommodating intraocular lenses versus mini-monovision with a monofocal intraocular lens. J Cataract Refract Surg 2013;39:48–55.
18. Szigeti A, Kránitz K, Takacs AI, et al. Comparison of long-term visual outcome and IOL position with a single-optic accommodating IOL after 5.5- or 6.0-mm femtosecond laser capsulotomy. J Refract Surg 2012;28:609–13.
19. Alió JL, Plaza-Puche AB, Montalban R, Ortega P. Near visual outcomes with single-optic and dual-optic accommodating intraocular lenses. J Cataract Refract Surg 2012;38:1568–75.
20. Tahir HJ, Tong JL, Geissler S, et al. Effects of accommodation training on accommodation and depth of focus in an eye implanted with a Crystalens intraocular lens. J Refract Surg 2010;26:772–9.
21. Brown D, Dougherty P, Gills JP, et al. Functional reading acuity and performance: comparison of 2 accommodating intraocular lenses. J Cataract Refract Surg 2009;35:1711–4.
22. Leydolt C, Neumayer T, Prinz A, Findl O. Effect of patient motivation on near vision in pseudophakic patients. Am J Ophthalmol 2009;147:398–405.
23. Marchini G, Pedrotti E, Sartori P, Tosi R. Ultrasound biomicroscopic changes during accommodation in eyes with accommodating intraocular lenses: pilot study and hypothesis for the mechanism of accommodation. J Cataract Refract Surg 2004;30:2476–82.
24. Stachs O, Schneider H, Beck R, Guthoff R. Pharmacological-induced haptic changes and the accommodative performance in patients with the AT-45 accommodative IOL. J Refract Surg 2006;22:145–50.
25. Stachs O, Schneider H, Stave J, Guthoff R. Potentially accommodating intraocular lenses—an in vitro and in vivo study using three-dimensional high-frequency ultrasound. J Refract Surg 2005;21:37–45.
26. Findl O, Drexler W, Menapace R, et al. High precision biometry of pseudophakic eyes using partial coherence interferometry. J Cataract Refract Surg 1998;24:1087–93.
27. Koeppl C, Findl O, Menapace R, et al. Pilocarpine-induced shift of an accommodating intraocular lens: AT-45 Crystalens. J Cataract Refract Surg 2005;31:1290–7.
28. Kriechbaum K, Findl O, Koeppl C, et al. Stimulus-driven versus pilocarpine-induced biometric changes in pseudophakic eyes. Ophthalmology 2005;112:453–9.
29. Yuen L, Trattler W, Boxer Wachler BS. Two cases of Z syndrome with the Crystalens after uneventful cataract surgery. J Cataract Refract Surg 2008;34:1986–9.
30. Cazal J, Lavin-Dapena C, Marín J, Verges C. Accommodative intraocular lens tilting. Am J Ophthalmol 2005;140:341–4.
31. de Castro A, Rosales P, Marcos S. Tilt and decentration of intraocular lenses in vivo from Purkinje and Scheimpflug imaging: validation study. J Cataract Refract Surg 2007;33:418–29.
32. Rosales P, Marcos S. Phakometry and lens tilt and decentration using a custom-developed Purkinje imaging apparatus: validation and measurements. J Opt Soc Am A Opt Image Sci Vis 2006;23:509–20.
33. Rosales P, Marcos S. Pentacam Scheimpflug quantitative imaging of the crystalline lens and intraocular lens. J Refract Surg 2009;25:421–8.
34. Grulkowski I, Gora M, Szkulmowski M, et al. Anterior segment imaging with Spectral OCT system using a high-speed CMOS camera. Opt Express [serial online] 2009;17:4842–58. Available at: http://www.opticsinfobase.org/oe/fulltext.cfm?uri=oe-17-6-4842&id=177259. Accessed June 11, 2013.
35. Grulkowski I, Liu JJ, Potsaid B, et al. Retinal, anterior segment and full eye imaging using ultrahigh speed swept source OCT with vertical-cavity surface emitting lasers. Biomed Opt Express [serial online] 2012;3:2733–51. Available at: http://www.opticsinfobase.org/boe/fulltext.cfm?uri=boe-3-11-2733&id=243196. Accessed June 11, 2013.
36. Ortiz S, Siedlecki D, Remon L, Marcos S. Optical coherence tomography for quantitative surface topography. Appl Opt 2009;48:6708–15.
37. Ortiz S, Siedlecki D, Grulkowski I, et al. Optical distortion correction in optical coherence tomography for quantitative ocular anterior segment by three-dimensional imaging. Opt Express [serial online] 2010;18:2782–96. Available at: http://www.opticsinfobase.org/oe/fulltext.cfm?uri=oe-18-3-2782&id=195232. Accessed June 11, 2013.
38. Ortiz S, Siedlecki D, Pérez-Merino P, et al. Corneal topography from spectral optical coherence tomography (sOCT). Biomed Opt Express [serial online] 2011;2:3232–47. Available at: http://www.opticsinfobase.org/boe/fulltext.cfm?uri=boe-2-12-3232&id=224150. Accessed June 11, 2013.
39. Ortiz S, Pérez-Merino P, Alejandre N, et al. Quantitative OCT-based corneal topography in keratoconus with intracorneal ring segments. Biomed Opt Express [serial online] 2012;3:814–24. Available at: http://www.opticsinfobase.org/boe/fulltext.cfm?uri=boe-3-5-814&id=231675. Accessed June 11, 2013.
40. Ortiz S, Pérez-Merino P, Gambra E, et al. In vivo human crystalline lens topography. Biomed Opt Express [serial

online] 2012;3:2471–88. Available at: http://www.opticsinfobase.org/boe/fulltext.cfm?uri=boe-3-10-2471&id=241405. Accessed June 11, 2013.
41. Ortiz S, Pérez-Merino P, Durán S, et al. Full OCT anterior segment biometry: an application in cataract surgery. Biomed Opt Express [serial online] 2013;4:387–96. Available at: http://www.opticsinfobase.org/boe/fulltext.cfm?uri=boe-4-3-387&id=248869. Accessed June 11, 2013.
42. Rosales P, Marcos S. Customized computer models of eyes with intraocular lenses. Opt Express [serial online] 2007;15:2204–18. Available at: http://www.opticsinfobase.org/oe/fulltext.cfm?uri=oe-15-5-2204&id=130575. Accessed June 11, 2013.
43. Gambra E, Sawides L, Dorronsoro C, Marcos S. Accommodative lag and fluctuations when optical aberrations are manipulated. J Vis 2009;9:1–15.
44. Rosales P, Wendt M, Marcos S, Glasser A. Changes in crystalline lens radii of curvature and lens tilt and decentration during dynamic accommodation in rhesus monkeys. J Vis 2008;18:1–12.
45. Radhakrishnan H, Charman WN. Age-related changes in static accommodation and accommodative miosis. Ophthalmic Physiol Opt 2007;27:342–52.
46. Olsen T. Prediction of the effective postoperative (intraocular lens) anterior chamber depth. J Cataract Refract Surg 2006;32:419–24.

Footnotes and Financial Disclosures

Originally received: March 8, 2013.
Final revision: June 13, 2013.
Accepted: June 13, 2013.
Available online: August 13, 2013. Manuscript no. 2013-373

[1] Instituto de Óptica "Daza de Valdés," Consejo Superior de Investigaciones Científicas, Madrid, Spain.

[2] Fundación Jiménez Díaz, Madrid, Spain.

Financial Disclosure(s):
Spanish patent: P201130685 (S.O. and S.M.).
The research leading to these results has received funding from the European Research Council under the European Union's Seventh Framework Programme (FP7/2007-2013) / ERC Grant Agreement n° 294099. Also, it has been suported by FIS2011-25637 (Spanish Goverment Grant) and the Consejo Superior de Investigaciones Científicas "Junta para la Ampliación de Estudios (JAE Pre to J.B). The authors also acknowledge Unidad Asociada Instituto de Óptica-Cosejo Superior de Investigaciones Científicas/FJD.

Correspondence:
Susana Marcos, PhD, Instituto de Óptica "Daza de Valdés," Consejo Superior de Investigaciones Científicas, C/Serrano, 121, 28006 Madrid, Spain. E-mail: susana@io.cfmac.csic.es.